Per-pixel energy calibration of photon counting detectors

2017 JINST 12 C03085

(http://iopscience.iop.org/1748-0221/12/03/C03085)

Published by IOP Publishing for Sissa Medialab

Received: *October 23, 2016*
Revised: *February 2, 2017*
Accepted: *February 27, 2017*
Published: *March 27, 2017*

18th International Workshop on Radiation Imaging Detectors
3–7 July 2016,
Barcelona, Spain

Per-pixel energy calibration of photon counting detectors

A. Atharifard,[a,1] **J.L. Healy,**[b] **B.P. Goulter,**[c] **M. Ramyar,**[a] **L. Vanden Broeke,**[d] **M.F. Walsh,**[c] **C.C. Onyema,**[d] **R.K. Panta,**[a,c] **R. Aamir,**[a,c] **D.J. Smithies,**[c] **R. Doesburg,**[c] **M. Anjomrouz,**[a] **M. Shamshad,**[a] **S. Bheesette**[a,f] **K. Rajendran,**[a] **N.J.A. de Ruiter,**[a,c,e] **D. Knight,**[a] **A. Chernoglazov,**[c,e] **H. Mandalika,**[e] **S.T. Bell,**[c,f] **C.J. Bateman,**[a,c,d] **A.P.H. Butler**[a,c,d,f] **and P.H. Butler**[c,d,f]

[a] *Department of Radiology, University of Otago, Christchurch, 2 Riccarton Ave, Christchurch 8140, New Zealand*
[b] *Department of Biology, University of Canterbury, Private Bag 4800, Christchurch 8140, New Zealand*
[c] *MARS Bioimaging Ltd, 29a Clyde Rd, Christchurch, New Zealand*
[d] *Department of Physics and Astronomy, University of Canterbury, Private Bag 4800, Christchurch 8140, New Zealand*
[e] *HIT lab NZ, Christchurch, New Zealand*
[f] *European Organization for Nuclear Research (CERN), Geneva, Switzerland*

E-mail: ali.atharifard@postgrad.otago.ac.nz

Abstract: Energy resolving performance of spectral CT systems is influenced by the accuracy of the detector's energy calibration. Global energy calibration maps a given threshold to the average energy response of all pixels of the detector. Variations arising from CMOS manufacturing processes and properties of the sensor cause different pixels to respond differently to photons of the same energy. Threshold dispersion adversely affects spectral imaging by degrading energy resolution, which contributes to blurring of the energy information.

In this paper, we present a technique for per-pixel energy calibration of photon-counting x-ray detectors (PCXDs) that quantifies the energy response of individual pixels relative to the average response. This technique takes advantage of the measurements made by an equalized chip. It uses a known global energy map to quantify the effect of threshold dispersion on the energy response of the detector pixels across an energy range of interest.

The proposed technique was assessed using a MARS scanner with an equalized Medipix3RX chip flip-bonded to 2 mm thick CdTe semiconductor crystal at a pitch of 110 μm. Measurements were made of characteristic x-rays of a molybdenum foil. Results were compared between the case

[1] Corresponding author.

doi:10.1088/1748-0221/12/03/C03085

that the global calibration was used on its own and the case of using it in conjunction with our per-pixel calibration technique. The proposed technique quantified up to 1.87 keV error in energy response of 100 pixels of a selected region of interest (ROI). It made an improvement of 28.3% in average FWHM. The additional information provided by this per-pixel calibration technique can be used to improve spectral reconstruction.

KEYWORDS: Computerized Tomography (CT) and Computed Radiography (CR); Data processing methods; Image filtering; Detector modelling and simulations II (electric fields, charge transport, multiplication and induction, pulse formation, electron emission, etc)

2017 JINST 12 C03085

Contents

2017 JINST 12 C03085

1 Introduction

Photon counting x-ray detectors (PCXDs) play a significant role in clinical imaging and examination of fatal disease [1]. Unlike other x-ray detectors, a PCXD can measure x-ray attenuation coefficients of materials across an energy range of interest in a single exposure. Therefore, a PCXD is capable of resolving energy levels of incident photons, and offers non-invasive characterization and identification of chemical components of materials [2].

To improve specificity of tissue characterization and material differentiation, an accurate selection of the energy range for measuring the difference in the attenuation of x-rays is required. This needs a correct identification of photon energies. Each detector pixel of a PCXD has separate electronics that can measure energy of the incident photons. Thus, every pixel can be considered as a small detector that needs to be calibrated. To achieve this, the output pulse amplitude of the ASIC is mapped to the associated photon energy [3], a process known as energy calibration.

Several energy calibration techniques employ monochromatic x-ray sources such as synchrotrons [4], radio-isotopes [5] and x-ray fluorescence (XRF) of metallic targets [6]. Some systems are not configured to adopt monochromatic sources, and in some cases, maintaining the proper geometry of the system needs a large space. Also, a long time may be required to set up the equipment before the measurements can be made. Therefore, these methods may not be practical for routine use in research and clinical environments.

Other methods of energy calibration use known reference energies. X-ray tube voltage was introduced as a reference energy for a practical and efficient energy calibration method [7, 8]. Although this technique was performed in an actual imaging system without using any other

measuring devices, it is not pixel specific, and cannot be used for calibration of individual pixels. However, we use this method as a preliminary calibration method in our experiments. In another method, a metallic foil is manually fastened on the detector to measure characteristic x-rays within the main beam [7]. The K_α energy of the foil element is related to the threshold at which maximum differential counts are registered by performing a threshold scan. Repeating the same experiment for several metallic foils results in a linear calibration map for the global thresholds. This technique measures XRF in presence of the main beam, therefore results are contaminated by bremsstrahlung. On the other hand, this method needs resources for employing foil elements that are appropriate for energy calibration. The reported methods do not address threshold dispersion that exists across the detector pixels. In this paper, a technique for calibrating pixels of PCXDs is described that takes into consideration differences in effective area of the pixels and accounts for inter-pixel threshold dispersion. To evaluate effectiveness of the technique, x-ray fluorescence of a molebdenum foil was measured outside of the main x-ray beams.

1.1 Medipix3RX detector

The Medipix3RX is an ASIC designed for spectroscopic imaging. It has adjustable low thresholds — i.e. only if the induced charge is above a given threshold, a local counter is incremented (figure 1a). Pixels of Medipix3RX can be operated in two different modes. In single pixel mode (SPM), each pixel has two thresholds and works independently of its adjacent pixels, hence charge sharing effect distorts the energy response of small detector pixels [9, 10]. To remove this effect, charge summing mode (CSM) of operation was introduced [10]. In this mode, clusters of four pixels are formed, providing 8 counters per cluster: four charge summing counters, three single pixel counters, and one arbitration counter. Deposited charge in each cluster is reconstructed through inter-pixel communication, and then arbitration counter assigns it to the pixel in which maximum portion of the charge was deposited.

2 Per-pixel energy calibration technique

In this study, we used the Medipix3RX chip in a MARS scanner [7, 9]. The chip was flip-bonded to 2 mm thick CdTe semiconductor crystal at a pitch of 110 μm^2. The detector was equalized using the electronic noise floor. The equalization process determines the noise floor as a level above the dark current noise of all pixels [11], therefore this type of noise is excluded from the measurements. In the following sections, the results are only shown for the first CSM counter (CSM_1). The methodology described here aims to measure the offset in true energy response of individual pixels relative to the global response. The global energy response of the detector is typically approximated by ($E_\gamma = m_g\, I_{\mathrm{DAC}} + c_g$) where E_γ is global energy response, I_{DAC} is one of 512 indices defined by 9 bits of the global DAC, and m_g and c_g are the slope and offset of the global energy calibration, respectively. Quantifying the offsets in the energy response for a pixel across the energy range (relative to the global response), gives a pixel-specific calibration map ($E_{\gamma,\mathrm{px}} = m_{\mathrm{px}}\, I_{\mathrm{DAC}} + c_{\mathrm{px}}$). m_{px} and c_{px} are the slope and offset of the true calibration map for that pixel, respectively, and are approximated using linear regression on the energy responses quantified at the target thresholds.

Figure 1b shows the flowchart of the technique in detail. Bad pixels are identified and filtered out prior to performing the calibration. Equally-spaced target energies are selected within the energy

2017 JINST 12 C03085

range of interest. For this study, we choose every 10 keV step across the range 20 keV to 110 keV. Sets of threshold scans are performed to acquire open-beam frames at the target thresholds, and then a set of energy offsets corresponding to effective count difference of each pixel is obtained across the spectrum.

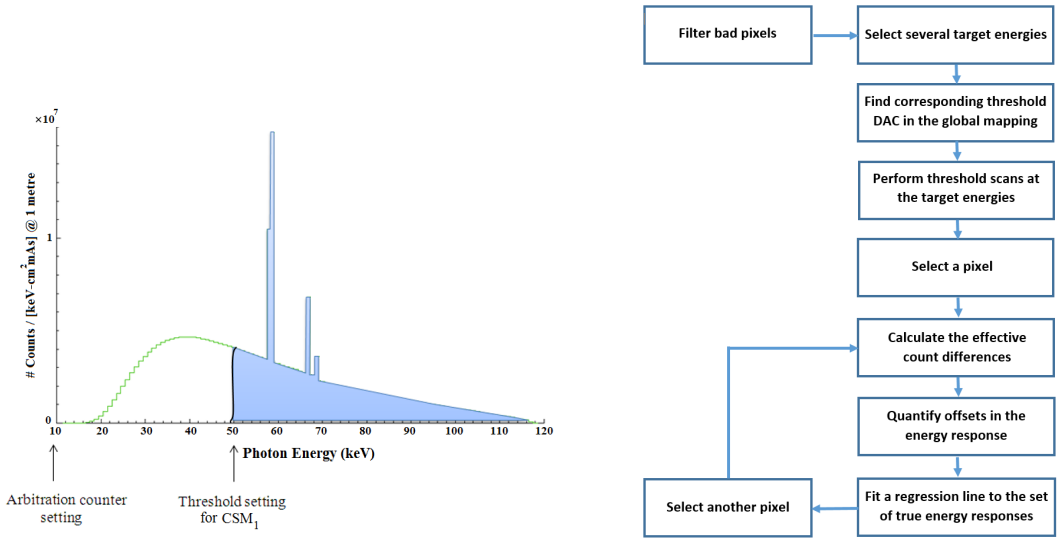

(a) **(b)**

Figure 1. (a) A low threshold counter measures all absorbed photons in a detector pixel that have an energy greater than or equal to a preset threshold. The arbitration counter is set above the noise floor and beneath the x-ray spectrum, providing an estimate of the total flux of the x-ray spectrum. (b) Flow chart of the proposed technique for per-pixel energy calibration of PCXDs.

2.1 Experimental setup and data acquisition

For the proposed per-pixel energy calibration technique, several datasets are acquired. At every target threshold, a threshold scan with step size of one is performed from two DAC values below to two DAC values above the selected target threshold. A tube voltage of 120 kVp, tube current of 30 μA (to avoid significant impact of co-incident photon pileup), and aluminum filtration of 1 mm (to attenuate low energy photons) are used for the measurements. To obtain sufficient samples for photon distribution, 200 frames are acquired at every threshold. In this paper, results are reported for a 10×10 region of interest (ROI) shown in figure 2a.

2.2 Pixel masking

Pixel masking is the process of identifying and filtering detector pixels that show either an inappropriate or no response to the incoming photons. Typically, three different types of bad pixels exist:

(i) *Dead pixels*: these pixels do not respond to the incoming signals. They are identified as pixels that consistently measure zero counts in a series of open beam measurements.

2017 JINST 12 C03085

(ii) *Over-counting pixels*: these are the pixels that record a number of photons in the dark field where there should be no signal as the x-ray source is switched off. Given the fact that all the measurements are made above the noise floor, pixels that count in the dark field are masked.

(iii) *Unstable pixels*: measurements obtained from good pixels are expected to be Poisson distributed [12]. Therefore pixels measuring with high level of uncertainty should be masked.

To filter unstable pixels, the following limit is applied:

$$C^f_{\text{var}} > (3 \times C^f_{\text{ave}}) \tag{2.1}$$

where C^f_{var} and C^f_{ave} are the variance and average of the measurements made by a pixel over 200 flat-field frames, respectively. Figure 2b shows pixel masking for the CdTe-Medipix3RX detector.

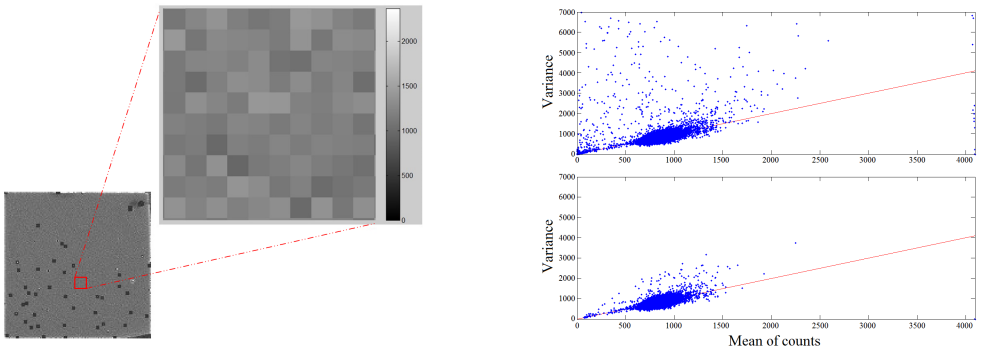

(a) **(b)**

Figure 2. (a) ROI of 100 pixels of CdTe-Medipix3RX selected for the measurements presented in this paper. (b) Variance against mean from 200 flat-field measurements; (top) before, and (bottom) after applying the pixel mask. Red lines represent Poisson distribution, and blue points represent average of measurements for individual pixels.

2.3 Effective count difference

As well as threshold dispersion, the absolute number of counts measured by a pixel is affected by its effective area. Hence, prior to attributing the measured counts to the energy thresholds, the dilation in counts from the effective pixel area needs to be taken into account. After the threshold equalization process, arbitration counters (C_{arb}) of all pixels are set to a level above the noise floor of all pixels [11]. However, measurements by C_{arb} show variations across the pixels due to variations in parameters of pixels' electronics and differences in effective area of the pixels. To cancel influence of the former effect, our technique compares measured counts by the arbitration counter of a pixel with the the counts recorded by a counter of the same pixel that is to be calibrated.

With C_{px} representing the average of absolute number of counts measured by a single pixel, $\overline{C}_{\text{arb}}$ and $\overline{C}$ are assumed to be average measurements of C_{arb} and C_{px} across the detector, respectively. If there was no threshold dispersion across the pixels, the effective area independent ratio of $C_{\text{px}}/C_{\text{arb}}$ would be equal to $\overline{C}/\overline{C}_{\text{arb}}$. Solving for the count recorded by a pixel gives

$$C_e = \overline{C} \times \frac{C_{\text{arb}}}{\overline{C}_{\text{arb}}} \tag{2.2}$$

2017 JINST 12 C03085

where C_e is the number of photons that the pixel is expected to measure. It is observed that for most pixels, the absolute number of counts, C_{px}, is not equal to C_e. Hence,

$$C_{\text{diff}} = C_e - C_{\text{px}} \tag{2.3}$$

where C_{diff} is the effective count difference that mostly originates from the offset in energy threshold of a pixel relative to global response.

2.4 Per-pixel energy mapping

Due to the concept of *low thresholds*, when a good pixel is counting higher than expected ($C_{\text{diff}} < 0$, according to eq. (2.3)), the true energy response of the pixel may be lower than the global energy response. Figure 3 illustrates measurements against energy thresholds based on the global energy mapping. Each point represents the average number of photons over 200 observations. The inset shows measurements of a 5-step threshold scan at the target energy of 30 keV (globally corresponding to threshold value of 80). This determines the ratio of number of counts to threshold at every target energy ($\Delta C/\Delta Th$). On the other hand, from the global energy calibration, approximated ratio of threshold to energy ($\Delta Th/\Delta E_\gamma$) is known. Therefore the rate of variations in measured counts to energy threshold is quantified as below

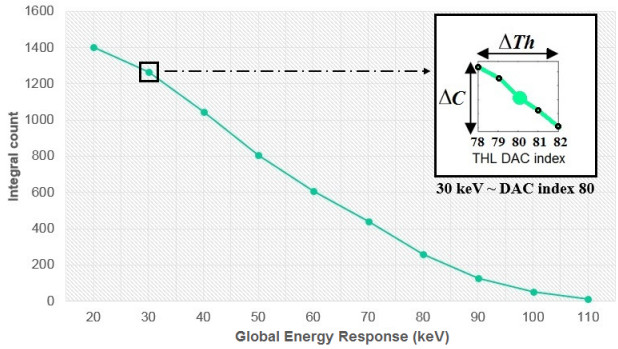

Figure 3. Investigation of $\Delta C/\Delta Th$ at selected target energies. The inset illustrates the 5-step threshold DAC scan at the target energy of 30 keV.

$$\frac{\Delta C}{\Delta E_\gamma} = \frac{\Delta C}{\Delta Th} \times \frac{\Delta Th}{\Delta E_\gamma} \tag{2.4}$$

Combining eq. (2.3) and eq. (2.4) gives

$$\Delta E_{\gamma,\text{px}} = C_{\text{diff}} \times \frac{\Delta E_\gamma}{\Delta C} \tag{2.5}$$

where $\Delta E_{\gamma,\text{px}}$ is the offset error for energy response of a pixel at an energy threshold of about E_γ. Repeating measurements for other target energies, gives a set of offsets that represents discrepancy between true energy response of a pixel, $E_{\gamma,\text{px}}$, relative to the global energy response. Therefore true energy response of a pixel at a target threshold is obtained as follows

$$E_{\gamma,\text{px}} = E_{\gamma,g} - \Delta E_{\gamma,\text{px}} \tag{2.6}$$

where $E_{\gamma,g}$ is the global energy response. To establish pixel-specific calibration maps, linear regression is applied to each set of true energy responses to their corresponding DAC values.

2017 JINST 12 C03085

3 Experimental analysis

The analysis presented in this section includes experimental results of the proposed per-pixel calibration technique that was used in conjunction with global energy calibration using the kVp method [7]. This is followed by the results of assessment of the technique. Figure 4 shows the global energy mapping (red) and energy mapping of the first 25 pixels in the ROI (blue). R^2 of linear regression was over 0.998 for various sets of energy response. Figure 5a indicates the true

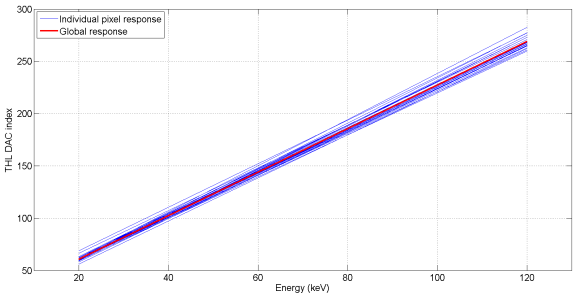

Figure 4. Global energy calibration map (red) by kVp method [7], and energy mapping of first 25 pixels of ROI (blue) quantified by our per-pixel calibration technique.

energy response of these pixels that were quantified by our technique when thresholds were globally set to 60 keV. Figure 5b shows that for only 100 pixels of the ROI, the amount of error in the global energy response varied between 1.38 keV and 1.87 keV.

3.1 Evaluation

Assessment of the proposed technique was carried out through measuring characteristic x-rays of a molybdenum foil using the setup proposed by [13]. The foil was placed in front of the source. After x-ray beams were attenuated by a 1 mm aluminum filter, the foil was exposed by the beam, and characteristic x-rays that emitted from the foil were captured by the detector outside of the main beam. An x-ray tube voltage of 40 kVp, anode current of 350 μA, exposure time of 1000 ms, and

58.04	61.36	61.81	60.84	61.57
61.71	60.42	59.16	59.89	60.87
62.46	60.34	59.00	58.72	58.18
58.39	56.50	60.14	60.04	60.08
56.59	57.43	60.12	57.86	62.16

(a)

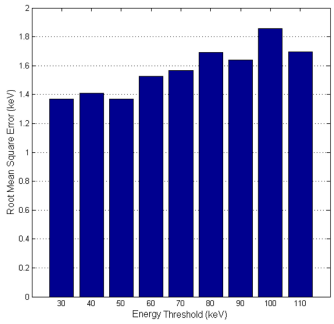

(b)

Figure 5. (a) True energy response of the pixels indicated in figure 4 when global setting was set to 60 keV. (b) RMSE of energy response across the energy spectrum for 100 pixels of the ROI.

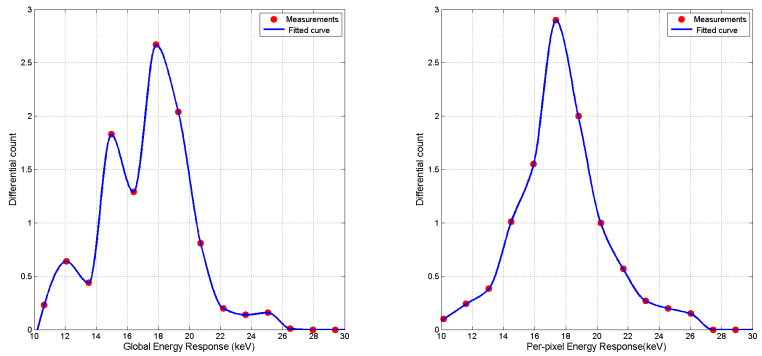

(a) **(b)**

Figure 6. Average response over 100 pixels of the ROI are shown for XRF Measurement via (a) global energy calibration (kVp method [7]), and (b) per-pixel energy calibration technique. The proposed technique improves average energy resolution of the detector by minimizing inter-pixel threshold dispersion.

source to detector distance of 150 mm were used. A threshold scan with step size of one DAC value was performed within a range of thresholds that contains molybdenum K_{α_1} energy, 17.48 keV. Using the global energy calibration, threshold DAC indices from 33 to 78 were determined to be a suitable range. To maintain both reasonable scan time and low quantum noise, 100 frames were acquired and averaged at every threshold. The differential spectrum was then obtained by taking numerical derivative with step size of three. Measurements are translated from DAC value to energy once according to global (average) energy response and the next time based on proposed per-pixel calibration technique. Figure 6 demonstrates a comparison between the measurements made according to the global energy calibration (left), and the same measurements when our proposed per-pixel calibration technique is applied (right). Note that each point represents average of only 100 pixels of the selected ROI. Our technique accounted for the inter-pixel threshold dispersion. This resulted in removing the undesired peaks and improved the average of FWHM by 28.3 % — i.e. equivalent to a reduction from 5.69 keV to 4.08 keV. In addition, the energy at which XRF was detected shifted to 0.53 keV lower energy and was detected at 17.36 keV instead of 17.89 keV with the global energy calibration.

4 Discussion

The aim of this study was to develop a pragmatic technique for per-pixel energy calibration of PCXDs. The proposed technique can be used in conjunction with any global calibration method. Prior to the technique, bad pixels need to be filtered out and threshold equalization is to be performed. To quantify energy response of individual pixels, our technique accounts for variations in electronics of detector channels, effective area of the pixels, and the inter-pixel threshold dispersion. It measures error in the global energy response across the pixel array. Results showed that threshold dispersion was minimum at low energies (close to the noise floor), and the residual threshold dispersion was more noticeable at higher energies (figure 4 and figure 5b). The rising trend of the error with energy was expected as prior to the measurements thresholds were equalized at the noise floor.

2017 JINST 12 C03085

Assessment of our per-pixel energy calibration technique demonstrated that it has the potential to obtain more accurate material information by improving energy resolution. This technique is expected to approximate the true energy response of the detector pixels, however as figure 6b indicates, there is still a small error in measuring energy of Mo fluorescence. This could be due to the charge sharing effect. Although we used the detector in charge summing mode, there could be still a chance that this effect causes a single event to be observed as two low energy counts. For the CdTe-Medipix3RX detector used for this study, since we used a Mo foil, characteristic x-rays of Cd and Te did not affect our measurements. However, as the mean free path length of K-fluorescence photons of Cd and Te are comparable (119 μm and 62 μm, respectively) with the dimension of the pixels (110 μm), if a foil element with higher K_α than K-edge of sensor materials was used, K-fluorescence photons of Cd and Te could be reabsorbed away from the original site where they were created. This can cause distortion of energy spectrum measured by the pixels.

This technique does not account for variations in the intensity of the x-rays that are incident on the detector. However, the MARS x-ray source model [14] shows that with the experimental setup used for our study, these variations had negligible effect on the measurements. In addition, pulse pileup which is a degrading factor in spectral CT could not affect our measurements for two reasons: measurements with global energy calibration were made at very low count rates, and the proposed technique measured XRF outside of the main beam that prevented the detector from being exposed by a high photon flux. One should notice that pileup can affect the measurements if a high flux rate of x-rays is used for the global energy calibration employed in conjunction with our technique.

Our analysis with a CdTe-Medipix3RX revealed ability of our technique to measure an RMSE of 1.38 keV to 1.87 ke$V$ (across the energy range) in the global energy response of pixels for a small ROI of 100 pixels. It quantified up to 6 keV energy threshold difference between two adjacent pixels when the global energy calibration was used (figure 5b). One should notice that an average FWHM of 4.08 keV was reported in this paper to show the effectiveness of the proposed technique in comparison with the global calibration method. However, this is not a value for the energy resolution of our system as several fluorescence lines are overlapped in the measurements. Our future focus will be on developing a fast and effective methodology that measures pixels' energy response independent from other calibration methods, so the above-mentioned conditions are easier to control.

5 Conclusions

We have presented a methodology for per-pixel energy calibration of PCXDs. Our technique used a previously introduced global energy calibration method to approximate the target thresholds. Considering the effective area of pixels, we quantified the true energy response of every pixel at a number of target thresholds, and a separate calibration map was then obtained for every detector pixel. Assessments using XRF measurements demonstrated that our technique can significantly enhance the energy resolution of the PCXDs. We are working towards using the information provided by this calibration technique to improve the results of spectral image processing techniques.

2017 JINST 12 C03085

References

[1] P. He, B. Wei, W. Cong and G. Wang, *Optimization of k-edge imaging with spectral CT*, *Med. Phys.* **39** (2012) 6572.

[2] X. Wang, D. Meier, S. Mikkelsen, G. Maehlum, D.J. Wagenaar, B. Tsui et al., *Micro CT with energy-resolved photon-counting detectors*, *Phys. Med. Biol.* **56** (2011) 2791.

[3] J.S. Lee, D.G. Kang, S.O. Jin, I. Kim and S.Y. Lee, *Energy calibration of a CdTe photon counting spectral detector with consideration of its non-convergent behavior*, *Sensors* **16** (2016) 518.

[4] E. Gimenez, R. Ballabriga, M. Campbell, I. Horswell, X. Llopart, J. Marchal et al., *Characterization of Medipix3 with synchrotron radiation*, *IEEE Trans. Nucl. Sci.* **58** (2011) 323.

[5] T. Koenig, J. Schulze, M. Zuber, K. Rink, J. Butzer, E. Hamann et al., *Imaging properties of small-pixel spectroscopic x-ray detectors based on cadmium telluride sensors*, *Phys. Med. Biol.* **57** (2012) 6743.

[6] J. Uher, G. Harvey and J. Jakubek, *X-ray fluorescence imaging with the Medipix2 single-photon counting detector*, in *IEEE Nuclear Science Symposuim & Medical Imaging Conference*, Knoxville, TN, 2010, pp. 1067–1073.

[7] R.K. Panta, M.F. Walsh, S.T. Bell, N.G. Anderson, A.P. Butler and P.H. Butler, *Energy calibration of the pixels of spectral x-ray detectors*, *IEEE Trans. Med. Imag.* **34** (2015) 697.

[8] M. Das, B. Kandel, C.S. Park and Z. Liang, *Energy calibration of photon counting detectors using x-ray tube potential as a reference for material decomposition applications*, *Proc. SPIE* **9412** (2015) 941214.

[9] R. Ballabriga, J. Alozy, G. Blaj, M. Campbell, M. Fiederle, E. Frojdh et al., *The Medipix3RX: A high resolution, zero dead-time pixel detector readout chip allowing spectroscopic imaging*, 2013 *JINST* **8** C02016.

[10] T. Koenig, E. Hamann, S. Procz, R. Ballabriga, A. Cecilia, M. Zuber et al., *Charge summing in spectroscopic x-ray detectors with high-Z sensors*, *IEEE Trans. Nucl. Sci.* **60** (2013) 4713.

[11] M.F. Walsh, *Spectral computed tomography development*, Ph.D. Thesis, University of Otago (2014).

[12] R.D. Yates and D.J. Goodman, *Probability and stochastic processes. a friendly introduction for electrical and computer engineering*, John Wiley & Sons (1999).

[13] L. Vanden Broeke, A. Atharifard, B.P. Goulter, J.L. Healy, M. Ramyar, R.K. Panta et al., *Oblique fluorescence in a MARS scanner with a CdTe-Medipix3RX*, 2016 *JINST* **11** C12063.

[14] M. Shamshad, M. Anjomrouz, D.J. Smithies, A. Largeau, G. Lu, A. Atharifard et al., *Semi-analytic x-ray source model for mars spectral CT*, submitted to *IEEE Trans. Med. Imag.*

2017 JINST 12 C03085